Korean Journal of Remote Sensing, Vol.24, No.5, 2008, pp.525~533

Fitting to Panchromatic Image for Pansharpening Combining Point-Jacobian MAP Estimation

Sang-Hoon Lee †

Kyungwon University, Korea

Abstract : This study presents a pansharpening method, so called FitPAN, to synthesize multispectral images at a higher resolution by exploiting a high-resolution image acquired in panchromatic modality. FitPAN is a modified version of the quadratic programming approach proposed in (Lee, 2008), which is designed to generate synthesized multispectral images similar to the multispectral images that would have been observed by the corresponding sensor at the same high resolution. The proposed scheme aims at reconstructing the multispectral images at the higher resolution with as less spectral distortion as possible. This study also proposes a sharpening process to eliminate some distortions appeared in the fused image of the higher resolution. It employs the Point-Jacobian MAP iteration utilizing the contextual information of the original panchromatic image. In this study, the new method was applied to the IKONOS 1m panchromatic and 4m multispectral data, and the results were compared with them of several current approaches. Experimental results demonstrate that the proposed scheme can achieve significant improvement in both spectral and block distortion.

Key Words : Image Fusion, Pansharpening, Regression Model, Block Distortion.

1. Introduction

In order to obtain valuable information on the ground from remotely sensed data, sufficiently high spatial resolution is required for detailed structure on ground surface and it is also necessary for detection of complex features to integrate abundant spectral information. Up to now the satellite imagery with very-high resolution of less than or equal to 1m resolution can be obtained from panchromatic sensors, while multispectral data are available only with mid-high or moderate spatial resolution. Image fusion techniques can effectively integrate the spatial detail of panchromatic data and the spectral characteristics of multispectral images. It is important for human's visual interpretation or computer's autonomous recognition to improve the accuracy in analyzing land-cover types.

The techniques to integrate panchromatic and multispectral data have mainly been developed for the application to generate RGB images of the higher spatial resolution of the panchromatic image. For this application, the IHS technique (Chavez and Anderson, 1991) and Brovey transform (Civco *et al.*,

Received October 10, 2008; Revised October 18, 2008; Accepted October 25, 2008.

† Corresponding Author: Sang-Hoon Lee (shl@kyungwon.ac.kr)

1995) have been most widely used in practice. The fusion techniques have been designed to obtain the synthetic images similar to the multispectral images that would have been observed from a sensor of the higher resolution. The synthesis process of multispectral images to the higher resolution of the panchromatic image is called "pansharpening" of multispectral images. Zhang and Hong (2005) assorted the algorithms for pansharpening into three categories: 1) projection and substitution methods, such as IHS technique 2) band ratio and arithmetic combination, such as Brovey Transformation, and 3) fusion method which injects spatial features of a panchromatic image into multispectral images. The injection method was earlier developed by using high-pass filtering to extract the spatial features, and later multiresolution analysis such as wavelet and Laplacian pyramids (Yocky, 1995; Nunez *et al.*, 1999; Aiazzi *et al.*, 2002) has been employed for detail injection. The eight algorithms recently developed and provided by seven research teams were compared with a standardized evaluation procedure (Alparone *et al.*, 2006). In their experiments, two algorithms, generalized Laplacian pyramid with context-based decision method (Aiazzi *et al.*, 2006) and additive wavelet luminance proportional method (Otazu, *et al.*), outperformed all others. They showed that the algorithms based on multiresolution analysis generally performed better than ones based on component substitution.

Most recently, the quadratic programming method was suggested to generate the synthesis of multispectral image at the higher resolution of the panchromatic image, which agrees with the observed spectral values (Lee, 2008). This scheme reconstructs the multispectral image at the higher resolution using the regression model fitting the panchromatic spectral values to the observed multispectral data. This study proposes a pansharpening method, FitPAN, which is a modified version of the quadratic programming method. It aims at minimizing or reducing the spectral distortion in the synthetic multispectral image of the higher resolution. However, the fusion process results in a block distortion at the boundary of the synthetic multispectral image. A sharpening process is also proposed to eliminate the block distortion using the contextual information of the panchromatic image and the Point-Jacobian MAP iteration (Lee, 2007). The new method was applied to the IKONOS 1m panchromatic image of 2400×2400 and 4m multispectral images of 600×600 acquired over the area around Anyang City of Korea.

2. Pansharpening by Fitting Panchromatic Image: FitPAN

Let z_j be the multispectral vector of the jth pixel in the synthetic image similar to the multiband image that would have been observed from a multispectral sensor with the higher resolution of the panchromatic image. The image model is usually assumed to be additive Gaussian. Under this assumption, given μ_j and Σ_j as the mean multispectral vector and its covariance matrix of the jth pixel in the multispectral image at the higher resolution, the objective function for the maximum likelihood estimates of $\{z_j\}$ is:

$$\underset{\{z_j\}}{\text{Max}} \left[\prod_{\forall_j} \Pr(z_j \mid \mu_j, \Sigma_j) \right]. \tag{1}$$

In the fusion, it is supposed that one pixel of the lower resolution can be divided into k^2 pixels of the higher resolution for an integer k. If $K = k^2$ and the $i(j)$ th pixel means the jth pixel of the higher resolution belonging to the ith pixel in the lower resolution,

$$\prod_{\forall_j} \left[\underset{\{z_{i(j)}\}}{\text{Max}} \left[\prod_{j=1}^{K} \Pr(z_{i(j)} \mid \mu_{i(j)}, \Sigma_{i(j)}) \right] \right]. \tag{2}$$

The optimization of Eq. (2) can be considered

independently for each pixel of the lower resolution, and equivalently,

$$\underset{\{z_{i(j)}\}}{\text{Max}} \sum_{j=1}^{K} (z_{i(j)} - \mu_{i(j)})^T \Sigma_{i(j)}^{-1} (z_{i(j)} - \mu_{i(j)}), \ \forall i. \quad (3)$$

In image processing, it is supposed that the intensity of each pixel corresponds to the average brightness which arises from the random emission of discrete particles (called photons) with identical energy. In terms of the number of photons, the spectral response of a pixel in the lower resolution is assumed to be equal to the average response of the pixels belonging to the corresponding area in the higher resolution at a same wavelength. For this assumption, the objective of Eq. (3) must be subject to:

$$\frac{1}{K} \sum_{j=1}^{K} z_{i(j)} = z_i^{Low}. \quad (4)$$

where z_i^{Low} is the observed multispectral vector of the ith pixel in the lower resolution. If the covariance matrix of multispectral vector is constant in a same pixel of the lower resolution, the optimization problem for the maximum likelihood estimates of $\{z_j\}$ can be restated using a Lagrangian coefficient vector:

$$\underset{\{z_{i(j)}\}}{\text{Max}} \sum_{j=1}^{K} \frac{1}{2} (z_{i(j)} - \mu_{i(j)})^T \Sigma_i^{-1} (z_{i(j)} - \mu_{i(j)}) + \lambda^T (K z_i^{Low} - \sum_{j=1}^{K} z_{i(j)}) \quad (5)$$

The optimal solution is obtained by solving a linear equation system of the first derivatives with respect to $\{z_{i(j)}\}$ and λ in Eq. (5):

$$\hat{z}_{i(j)} = \mu_{i(j)} + (z_i^{Low} - \bar{\mu}_i), j = 1,2,\cdots, K. \quad (6)$$

The true mean vectors, $\{\mu_{i(j)}\}$, are not known in most application. Lee (2008) suggested that the mean vector can be estimated based on the observation using a polynomial regression model of order p:

$$\mu_{i(j)} = \sum_{k=0}^{p} \beta_k x_{i(j)}^k. \quad (7)$$

where $x_{i(j)}$ is the observed value of the $i(j)$ th pixel from the higher resolution sensor and β_k are the kth polynomial coefficient vector. From Eqs. (6) and (7), a pansharpening scheme, so called FitPAN, is established:

$$\begin{bmatrix} \hat{B}_{i(j)} \\ \hat{G}_{i(j)} \\ \hat{R}_{i(j)} \\ \hat{Nir}_{i(j)} \end{bmatrix} = \begin{bmatrix} \hat{\mu}_B(P_{i(j)}) + \delta_i^B \\ \hat{\mu}_R(P_{i(j)}) + \delta_i^G \\ \hat{\mu}_G(P_{i(j)}) + \delta_i^R \\ \hat{\mu}_{Nir}(P_{i(j)}) + \delta_i^{Nir} \end{bmatrix} \quad (8)$$

$$\hat{\mu}_M(P_{i(j)}) = \sum_{k=0}^{p} \hat{\beta}_M^k P_{i(j)}^k$$

$$\delta_i^M = M_i - \frac{1}{K} \sum_{j=1}^{K} \mu_M(P_{i(j)})$$

where $P_{i(j)}$ is the $i(j)$ th pixel's value of panchromatic image of the higher resolution M_i and the ith pixel's value of M band multispectral image of the lower resolution.

3. Experimental Results and Evaluation for FitPAN

For evaluation of the fusion process, this experiment used IKONOS 1m panchromatic image of 2400×2400 and 4m multispectral images of 600×600 acquired over the area around Anyang City of Korea. The IKONOS data of unsigned 11bit range from 0 to 2047. The performance of FitPAN was compared to them of three current techniques:

1) Generalized IHS transformation (GIHS) (Carper *et al.*, 1990)
2) Gram-Schmit spectral sharpening method (GS) as implemented in ENVI (Laben and Brower, 2000)
3) Additive Wavelet Luminance Proportional (AWLP) (Nunez *et al.*, 1999)

To assess the quality of fused images with quantitative measurement, the panchromatic and multispectral images were first degraded to 4m and 16m respectively. The fusion methods were applied

to the degraded data and then generated the multispectral images of 4m resolution. The synthetic images were statistically compared with the original multispectral images. Wald *et al.* (1997) suggested three conditions which a good fused image should satisfy:

1) After that the fused image M_h^* is degraded to its original resolution, it should be as similar as possible to the original image M_l.
2) Any fused image M_h^* should be as identical as possible to the image that would have been observed from the corresponding sensor of the higher resolution.
3) The set of fused multispectral images should be as identical as possible to the set of multispectral images that would have been observed from the corresponding sensor of the higher resolution.

The proposed FitPAN satisfies the first condition perfectly because it optimized with the constraint of Eq. (4). The root mean square error (RMSE) and the correlation coefficient (CC) between M_l and M_h^* for (Nir, Red, Green, Blue) bands are employed to evaluate the second condition for the fused images:

$$RMSE(b) = \sqrt{\frac{1}{N_{pixel}} \sum_{\forall i(j)} (z^*_{i(j),b} - z_{i(j),b})^2} \qquad (9)$$

where $z_{i(j),b}$ and $z^*_{i(j),b}$ are the original and pansharpened values of the $i(j)$ th pixel at the bth band, N_{pixel} is the number of pixels in the higher resolution image, $Z_b = \{z_{i(j),b}\}$ and Z_b^* are the original and pansharpened image of the bth band, and σ_{Z_b} is the standard deviation of Z_b. The Q index defined in (Zhou and Bovik, 2002) is also stated as

$$Q(b) = \frac{4\mathrm{cov}(Z_b^*, Z_b)\mu_{Z_b^*}\mu_{Z_b}}{(\sigma^2_{Z_b^*} + \sigma^2_{Z_b})(\mu^2_{Z_b^*} + \mu^2_{Z_b})} \qquad (10)$$

where μ_{Z_b} is the mean of Z_b. The dynamic range of Q is [-1,1], and the best value Q = 1 iff $Z_b^* = Z_b$ for all pixel. To increase the discrimination capability in Eq. (10), all statistics are calculated on suitable image blocks and the resulting values of Q are averaged over the whole image to yield a unique global score.

The third condition is evaluated by three different indices of average cumulative quality/distortion. The first index is *ERGAS* (erreur relative globale adimensionelle de synthese), which means "dimensionless global relative error of synthesis," defined by

$$ERGAS = 100 Ratio_{l/h} \sqrt{\frac{1}{N_{band}} \sum_{\forall b} \left(\frac{RMSE(b)}{MEAN(b)}\right)^2} \qquad (11)$$

where $Ratio_{l/h}$ is the ratio of the lower resolution to the higher resolution, N_{band} is the number of bands, and $MEAN(b) = \sum_{\forall i(j)} z_{i(j),b}/N_{pixel}$ is the mean intensity of the original image of the bth band. The capability of *ERGAS* is to measure globally the radiometric distortion in fusion. The second index is based on the spectral angular mapper (*SAM*) which denotes the absolute value of the spectral angle between two intensity vectors:

$$SAM_{i(j)} = \cos^{-1}\left(\sum_b \frac{(z_{i(j),b}\, z^*_{i(j),b})}{\sqrt{(z^*_{i(j),b})^2}\sqrt{(z_{i(j),b})^2}} \right). \qquad (12)$$

A value of $SAM_{i(j)}$ equal to zero denotes absence of spectral distortion, but radiometric distortion is possible. the spectral angular mapper distortion is measured in degrees and averaged over the whole image to yield a global measurement of spectral distortion. The second index is then defined by

$$\overline{SAM}_{\deg} = \frac{180}{\pi} \frac{\sum_{\forall i(j)} SAM_{i(j)}}{N_{pixel}}. \qquad (13)$$

The $Q4$ index is a generalization of the Q index for multidimensional data. Let Z and Z^* denote the original and pansharpened image of four bands, respectively, expressed as quaternions:

$$Z = Nir + iR + jG + kB$$
$$Z^* = Nir^* + iR^* + jG^* + kB^* \qquad (14)$$

The $Q4$ index defined as

$$Q4 = \frac{4\mathrm{cov}(Z^*,Z)\,|\mu_{Z^*}||\mu_Z|}{(\sigma_Z^2+\sigma_Z^2)(|\mu_{Z^*}|^2+|\mu_Z|^2)}. \qquad (15)$$

considers both radiometric and spectral distortions. Same as for Eq. (10), ensemble expectations are calculated on suitable image blocks. Tables 1 - 4 show the results of evaluation measurement for the four pansharpening techniques. The Q and $Q4$ indices were calculated as averages on 8×8 blocks.

As shown in Tables 1 - 3, the statistical measures of spectral quality for FitPAN are considerably favourable compared to them for AWLP in the Red and Nir bands, but AWLP is comparable with FitPAN in the Blue and Green bands. Fig. 1 displays the scatter plots of the four multispectral values vs. the panchromatic values of IKONOS data used in this experiment. These plots used the panchromatic values coming from the image of 4m resolution which was degraded to the lower resolution of the multispectral image. The correlations between them are also show in Fig. 1 in parenthesis. The panchromatic data have larger correlations with the Red and Nir data than with the Blue and Green data as shown Fig. 1. For the Red and Nir bands, the estimated regression models of Eq. (7) then fit better to the observation, and FitPAN is supposed to result in less distortion by using the better estimate of the true mean vector. It was proved by the results of Tables 1 - 3. In overall evaluation to the results in Tables 1 - 4, it is clear that FitPAN generated the synthetic multispectral images of 1m resolution with less spectral and radiometric distortions than the other three techniques did. Fig. 2 shows the observed RGB sub-image of 75×75 and the corresponding panchromatic image of 300×300, and also shows the pansharpened RGB images generated by the four fusion techniques. It is not easy to distinguish visually quality of the resultant images.

Table 1. Root Mean Sqaure Errors between original multispectral image and pansharpened multispectral images of 4m resolution

RMSE	GIHS	GS	AWLP	FitPAN
B	241.68	115.96	89.47	92.62
G	237.91	130.02	92.09	89.99
R	241.58	145.40	113.64	99.48
Nir	228.74	137.02	119.77	92.39

Table 2. Correlation Coefficients between original multispectral image and pansharpened multispectral images of 4m resolution

CC	GIHS	GS	AWLP	FitPAN
B	0.8994	0.9201	0.9489	0.9476
G	0.9308	0.9298	0.9600	0.9628
R	0.9373	0.9295	0.9519	0.9620
Nir	0.9421	0.9237	0.9387	0.9616

Table 3. Q Index values computed from original multispectral image and pansharpened multispectral images of 4m resolution

Q	GIHS	GS	AWLP	FitPAN
B	0.8743	0.8949	0.9487	0.9466
G	0.9043	0.9004	0.9581	0.9623
R	0.9020	0.9027	0.9457	0.9618
Nir	0.8707	0.8970	0.9245	0.9588

Table 4. Average Cumulative Index values for distortions between original multispectral image and pansharpened multispectral images of 4m resolution

Index	GIHS	GS	AWLP	FitPAN
ERGAS	7.2463	4.1321	3.3621	2.8869
SAM	5.9385	4.5620	4.3542	3.8873
Q4	0.9028	0.9043	0.9452	0.9591

4. Block Distortion Correction

The experimental results of Section 3 show that FitPAN reduced the distortion of spectral information compared to the other methods. However, block distortion was appeared on the boundary in the synthetic multispectral image at the higher resolution of the panchromatic image. To correct this problem, a sharpening process of the Point-Jacobian Iteration

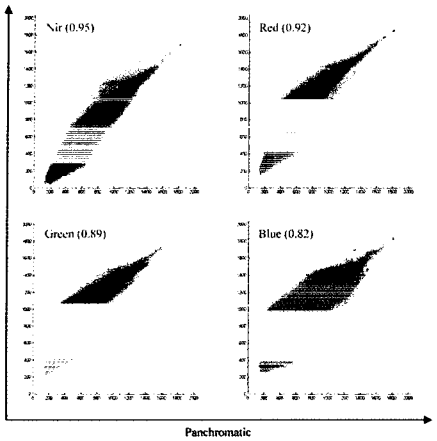

Fig. 1. Scatter plots of panchromatic value vs. multispectral value: correlation between panchromatic data and multispectral data in parenthesis (panchromatic image is degraded to the lower resolution of multispectral image).

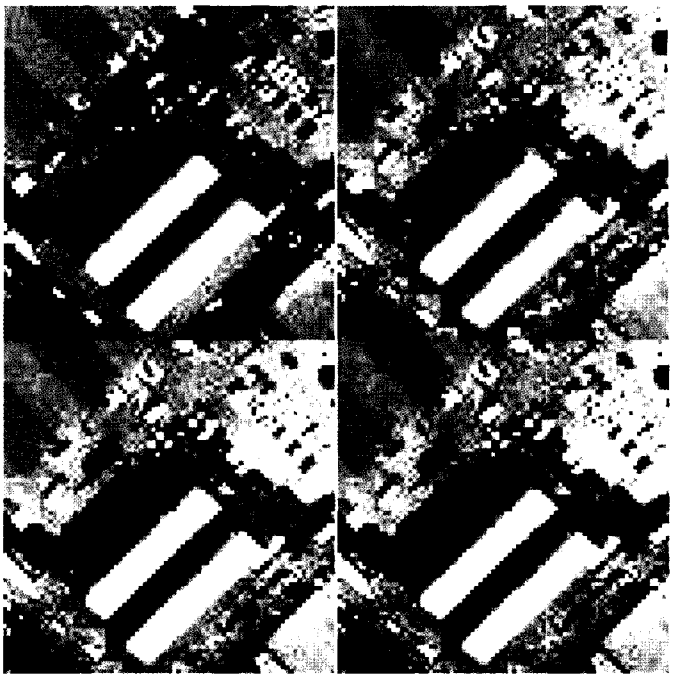

Fig. 3. Results of sharpening process to remove block distortion(original panchromatic image and FitPAN-fused image before sharpening process in the top line, FitPAN-fused images after sharpening process of 7×7 window with r = 0.5 and 2.0 respectively from left in the bottom line).

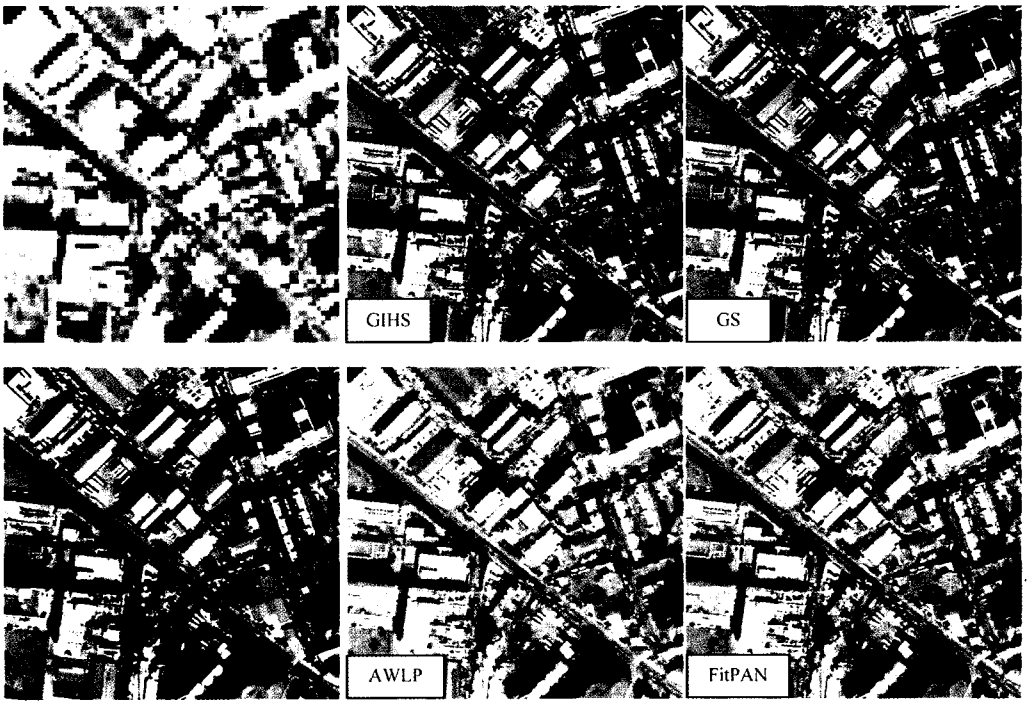

Fig. 2. Pansharpened images of 4 fusion techniques using RGB image of 4m resolution and panchromatic image of 1m resolution observed from IKONOS.

MAP (PJIMAP) estimation (Lee, 1991; Lee, 2007) is proposed in this study. The proposed scheme is designed to utilize the contextual information of the original panchromatic image.

Given an observed image Y, the Bayesian method is to find the MAP estimate from the mode of the posterior probability distribution of the original image X, or equivalently, to maximize the log-likelihood function. The log-likelihood function using a Gaussian image model and MRF texture model is:

$$lPN \propto -(Y-X)^T\Sigma^{-1}(Y-X) - X^T\mathbf{B}X \qquad (16)$$

where $\Sigma = diagonal\{\Sigma_i\}$ is the covariance matrix of the Gaussian image model and $\mathbf{B} = \{\beta_{ij}\}$ is the bonding strength matrix which is associated with local interaction between neighbouring pixels. If the bonding strength is only dependent on spatial location, β_{ij} is constant and $\mathbf{B} = \{\beta_{ij}\mathbf{I}_m\}$ where m is the number of bands and $\mathbf{I}_m$ is the m-dimensional identity matrix. Since the log-likelihood function is convex, the MAP estimate of X is obtained by taking the first derivative, and then using the Point-Jacobian iteration, the original image can be recovered iteratively: if each band has a same bonding strength, at the h th iteration (Lee, 1991)

$$\hat{x}_i^h = (\Sigma_i^{-1} + \beta_{ii})^{-1}\left(\Sigma_i^{-1}y_i - \sum_{(i,j)\in C_p}\beta_{ij}\hat{x}_j^{h-1}\right) \qquad (17)$$

where C_p is the pair-clique system of $\{I_n, R\}$ if a "neighbourhood system" for the image index system, I_n.

To correct block distortion in pansharpening, the bonding strength coefficients, β_{ij}, are estimated using the original panchromatic data. For $\hat{\beta}_{ij} = \hat{\phi}_i\hat{\alpha}_{ij}$ (Lee, 2007),

$$\hat{\phi}_i = \sqrt{\frac{r}{\sigma_i^2\sum_{(i,j)\in C_p}\hat{\alpha}_{ij}(P_i - P_j)^2}} \qquad (18)$$

$$\hat{\alpha}_{ij} = \begin{cases} \dfrac{(P_i - P_j)^{-2}}{\sum_{(i,k)\in C_p}(P_i - P_k)^{-2}} & \text{for (i,j)} \in C_p \\ 0 & \text{otherwise} \end{cases}$$

where P_i and σ_i^2 are the spectral value and variance of the ith pixel in the panchromatic image respectively. The bonding strength coefficients estimated from Eq. (18) represents local interaction between neighbouring pixels and can provide some contextual information on the local region in the panchromatic image. Given an initial vector, $\hat{x}_i^0 = y_i$ where $\{y_i\}$ is a synthetic multispectral image generated from pansharpening, the iteration of Eq. (17) generates an image $\{\hat{x}_i\}$ sharpened based on spatial texture of the panchromatic image.

For this sharpening process, r in Eq. (18) and the window size for the neighbourhood system should be determined. To examine the effect of these parameters on the results of the sharpening process, the experiment was performed with various values of r and the window size for the degraded images same as in the previous section. The sharpening process was applied to the FitPAN-fused image with significant block distortion as shown in Fig. 3. Table 5 shows the results of statistical measurement for quality of the synthetic data after sharpening the fused images to remove block distortion using the window size of 7×7 and various values of r. As r decreases, the statistical measurement slightly improves, but it is not significant for considering any change in image quality. Table 6 shows the results of statistical measurement for various window sizes with a fixed value of r. They also do not show any significant change according to the window size, but give an implication of the choice of the window size. It may be a better choice to use a window size which is approximately twice as large as the ratio of the higher resolution to the lower resolution. The sharpening process was next applied to the synthetic multispectral image of 1m resolution fused by FitPAN, and the results were investigated for quality by visual inspection. Fig. 3 also shows two images which enlarge a sub-area of the synthetic images after sharpening with $r = 0.5$ and 2.0 using the window size of 7×7. As shown in the figure, block distortion

Table 5. Average Cumulative Index values for distortions between original multispectral image and FitPAN-fused multispectral images of 4m resolution before and after sharpening process with various values of r for block distortion (window size = 7×7)

Index	Before	After				
		$r=2.0$	$r=1.0$	$r=0.5$	$r=0.1$	$r=0.01$
ERGAS	2.8869	2.9801	2.9547	2.9342	2.9033	2.8864
SAM	3.8873	3.9090	3.8859	3.8857	3.8722	3.8706
Q4	0.9591	0.9569	0.9576	0.9581	0.9588	0.9592

Table 6. Average Cumulative Index values for distortions between original multispectral image and FitPAN-fused multispectral images of 4m resolution before and after sharpening process with various window sizes for block distortion ($r=0.5$)

Index	Before	After				
		3×3	5×5	7×7	9×9	11×11
ERGAS	2.8869	2.9704	2.9463	2.9342	2.9375	2.9415
SAM	3.8873	3.9397	3.9015	3.8857	3.8880	3.8929
Q4	0.9574	0.95749	0.9579	0.9581	0.9579	0.9577

was disappeared by applying the proposed sharpening process. Even though it is hard to distinguish visually quality in two images, the result of r = 2.0 shows better quality in detailed inspection. It is suggested to use somewhat large value of r greater than 1.

5. Conclusions

The pansharpening method of multispectral image, FitPAN was proposed to reconstruct at the higher resolution the multispectral images which agree with the spectral values observed from the sensor of the lower resolution. In the proposed scheme, a regression model represents the relation between panchromatic and multispectral images, and is utilized to estimate the true mean vector of multispectral image of the higher resolution based on the multispectral observation. The pansharpening is constructed under the constraint that the spectral response of a pixel in the lower resolution is equal to the average response of the pixels belonging to the corresponding area in the higher resolution at a same wavelength. However, some block distortions were appeared in the synthetic multispectral image fused by FitPAN. The sharpening process proposed in this study effectively eliminated the block distortions using the contextual information of the panchromatic image without changing quality of the fused image.

Acknowledgement

This research was supported by a grant(code# 07KLSGC03) from Cutting-edge Urban Development - Korean Land Spatialization Research Project funded by Ministry of Construction & Transportation of Korean government.

References

Aiazzi, B., L. Alparone, S. Baronti, and A. Garzelli, 2002. Context-driven fusion of high spatial and spectral resolution images based on oversampled multiresolution analysis, *IEEE Trans. Geosci. Remote Sens.*, 40: 2300-2312.

Alparone, L., L. Wald, J. Chanussot, C. Thomas, P. Gamba, and L. M. Bruce, 2006. Comparison

of pansharpening algoriths: Outcome of the 2006 GRS-S data-fusion contest, *IEEE Trans. Geosci. Remote Sensing*, 45: 3012-3021.

Carper , W., T. Lillesand, and R. Kiefer, 1990. The use of intensity-hue-saturation transformations for merging Spot panchromatic and multispectral image data, *Photogram. Eng. Remote Sensing*, 56: 459-467.

Chavez, P. S., S. C. Sildes, and J. A. Anderson, 1991. Comparison of three different methods to merge multiresolution and multispectral data: Landsat TM and SPOT panchromatic, *Photogramm. Eng. Rem. Sens.*, 57: 295-303.

Civco, D. L., Y. Wang, and J. A. Silander, 1995. Characterizing forest ecosystems in Connecticut by integrating Landsat TM and SPOT panchromatic data, *Proc.1995 Annual ASPRS/ACSM Convention*, Charlotte, NC., 2: 216-224.

Laben, C. A.and B. V. Brower, 2000. Process for enhancing the spatial resoltion of multispectral imagery using pan-sharpening, Technical Report US Patent #6,110,875, Eastman Kodak Company.

Lee, S-H, 2007. Adaptive Iterative Despeckling of SAR Imagery, *Korean J. Remote sens.*, 23: 455-464.

Lee, S-H, 2008. Quadratic Programming Approach to Pansharpening of Multispectral Images Using a Regression Model, *Korean J. Remote sens.*, 24: 257-267.

Lee S. and M. M. Crawford, 1991. An Adaptive Reconstruction System for Spatially Correlated Multispectral Multitemporal Images, *IEEE Trans. Geosci. Remote Sens.*, 29: 494-508.

Nunez, J., X. Otazu, O. Fors, A. Prades, V. Pala, and R. Arbiol, 1999. Multiresolution-based image fusion with additive wavelet decomposition, *IEEE Trans. Geosci. Remote Sens.*, 37: 1204-1211.

Otazu, X., M. Gonzales Audicana, O. Fors, and J. Nunez, 2005. Introduction of sensor spectral response into image fusion methods: Application to wavelet-based methods, *IEEE Trans. Geosci. Remote Sens.*, 43: 2376-2385.

Wald, L., T. Ranchin, and M. Mangolini, 1997. Fusion of satellite images of different spatial resolutions: Assessing the quality of resulting images, *Photogramm. Eng. Remote Sens.*, 63: 691-699.

Yocky, D. A., 1996. Multiresolution wavelet decomposition image merger of landsat thematic mapper and spot panchromatic data, *Photogramm. Eng. Rem. Sens.*, 69: 1067-1074.

Zhang, Y and G. Hong, 2005. An IHS and wavelet integrated approach to improve pan-sharpening visual quality of natural colur IKONS and QuickBird images, *Information Fusion*, 6: 225-234.

Zhou W. and A.C. Bovik, 2002. A universal image quality index, *IEEE Signal Processing Lett.*, 9: 81-84.